The Effects of Dipole Twist on the Closed Orbit in RHIC

J. Milutinovic

March 1990

Collider Accelerator Department

Brookhaven National Laboratory

U.S. Department of Energy

USDOE Office of Science (SC)

DISCLAIMER

RHIC PROJECT

Brookhaven National Laboratory
Associated Universities, Inc.
Upton, NY 11973

The Effects of Dipole Twist on the Closed Orbit in RHIC

J. Milutinovic

March 1990

The Effects of Dipole Twist on the Closed Orbit in RHIC

J. Milutinovic

Accelerator Development Department

March 16, 1990

Abstract

We have examined the consequences of a dipole twist in the domain of closed orbit distortions and its correction in RHIC. To be specific, we impose the dipole twist as an extra disturbing factor on the previously analyzed and corrected orbit in RHIC, due to axial tilts and errors in the integrated field strength in dipoles and due to lateral displacements of quads. We have found out that even though in most cases the local three–bump correcting scheme can cope with rms values of the twist being in the vicinity of 10 mrad, there are still some cases where the scheme breaks down for the twist angle rms values as low as 4.5 mrad. On the basis of this experience, we recommend rejection of any dipole whose rms value of the twist angle exceeds 3.0 mrad.

Introduction

An accelerator lattice cannot expected to be perfect and as an immediate consequence the same will be true for the closed orbit and linear optics of the machine. The impact of lattice errors on the closed orbit was analyzed in the past by the author of this technical note, for several machines including RHIC, for which it remains a topic of current research interest. Since the details of the past investigations were reported in technical notes,[1] they will not be repeated here. However, we will mention the basic assumptions we made in the past investigations since we keep them unchanged in our present work.

---

[1] J. Milutinovic and A.G. Ruggiero, *Closed Orbit Analysis for RHIC*, Technical Note AD/RHIC–AP–78.

J. Milutinovic and A.G. Ruggiero, *Closed Orbit Analysis for RHIC*, Proc. 1989 IEEE Particle Accelerator Conference, IEEE 89CH2669–0, 1370.

Related useful background may be found in the following technical notes describing other machines.

J. Milutinovic and A.G. Ruggiero, *Closed Orbit Analysis for the AGS Booster*, Booster Technical Note No. 107, and references cited therein.

J. Milutinovic and A.G. Ruggiero, *Analysis of Effects of Closed Orbit Errors, Quadrupole $\Delta K/K$ Random Errors and Random Quadrupole Rotation Errors for the SSC LEB*, Accelerator Physics Technical Note No. 14.

Among many possible sources of orbit distortions, we selected four major types of lattice errors in our past investigations. They were the error in the integrated dipole field strength $\Delta(B\ell)/B\ell$, the axial tilt of the dipole $\Delta\theta$, and the lateral displacements of the quadrupole along the two transverse directions.

The rms values of the lattice errors we used were the following ones:

$$\Delta(B\ell)/B\ell = 0.5 \times 10^{-3}, \qquad \Delta\theta = 1.0 \times 10^{-3} \text{ radians,}$$

$$\text{Lateral quad displacements}: \quad \Delta_Q X = \Delta_Q Y = 0.25 \times 10^{-3} \text{ m .}$$

These rms values are currently accepted for RHIC and are independent of any kind of dipole twist, whose considerations came into play fairly recently. With the above displayed rms error values, and in the absence of twist, we found out that the local three–bump correcting scheme, such as that implemented at Fermilab, was capable of correcting orbit distortions down to acceptable values (i.e. < 1 mm) well within the strength capacities of the presently adopted orbit correcting hardware, which is supposed to be capable of delivering 0.3 T·m of integrated field strength.

The tracking/analysis code PATRIS was used in the past and present work to handle the simulation and analysis of closed orbit distortions and furthermore to correct them. A 2.5σ cut was imposed on all distributions of random errors used in the past and present simulations.

The lattice, chosen to simulate the effects of twist on closed orbit, was the currently adopted $\beta^* = 2$m lattice. This is because it is more sensitive to errors than the $\beta^* = 6$m lattice and is also more difficult to correct. Therefore, whatever remedy will be needed for the former it will also suffice for the latter.

As we already mentioned, no attention was paid in the past to the dipole twist, i.e. the variation of the direction of the main bending field within the dipole was absent from all simulations until recent times. This was probably so because of intuitive feeling that only the average bending field direction really matters. However, this feeling was shattered by the results of recent measurements of the field quality in the dipole, reported by P. Wanderer and E. Willen.[2] The variation of the direction of the dipole field along the magnet was found to be quite conspicuous (see Fig. 1) and prompted several researchers, including us, to investigate the impact of this twist on various characteristics of the machine.

---

[2] P. Wanderer and E. Willen, Magnet Test Group, MTG–439 (RHIC–34).
P.A. Thompson, RHIC Dipole DRC007, Technical Note RHIC–MD–93.

Modeling of the Twist

Magnet twist has been defined as the change of the direction of magnetic field along the magnet axis, i.e. along the longitudinal direction customarily labeled by the parameter s. Consequently, $\vec{B} = \vec{B}(s)$ and the usual assumption in deriving the equations of motion for tracking codes, $\vec{B} = $ const. in the dipole, is no longer valid. Compliance with the Maxwell equations now demands the presence of a solenoidal field component $B_s \neq 0$.

A proper procedure would be now to rederive the equations of motion, which would include the solenoidal field component, to integrate them for suitably chosen $\vec{B}(s) = \vec{B}(\alpha(s))$, where $\alpha(s)$ is the directional deviation of the dipole magnetic field from the vertical plane, to incorporate the solutions into the adopted tracking/analysis codes and simulate this on the computer. However, due to shortage of time and based on indications that the solenoidal field component is small,[3]   we decided to take a shortcut and to simulate the effects of magnet twist on the closed orbit by using only slightly modified existing software, i.e. with PATRIS.

The way we decided to simulate the twist was to introduce segmental rotations in the dipole, on top of the overall random rotation with the 1 mrad rms value, simulated in the past. This means that we divided each dipole into several segments which were first subjected to the same random rotation with the rms value over the whole lattice being 1 mrad (a Gaussian random distribution with a 2.5σ cut), and after that subjected to additional individual rotations, described by different sequences of random numbers, with rms values of these rotation angles to be determined in order to establish magnet tollerances, and with a 2.5σ cut as before. Three specific models have been considered.

Model 1. Dipole split into two segments. In this case the two segments were subjected to additional individual rotations which were totally uncorrelated (see Fig. 2).

Model 2. Dipole split into four segments. In this case the four segments were subjected to additional individual rotations which were totally uncorrelated (see Fig. 3).

Model 3. Dipole split into seven segments. In this case the seven segments were subjected to additional individual rotations which were not totally uncorrelated (see Fig. 4). The rotations were determined in the following manner. The two end sections and the whole block of three central segments were rotated by three completely random angles. The remaining two intermediate segments were rotated by the two angles which were found

---

[3] J. Claus, Private communication.
  J. Wei, Private communication.

3

by suitably interpolating the three basic random angles that rotated the end segments and the inner block. Finally, the single innermost segment received an extra rotation that mimicked the cusp found in magnet measurements (see Fig. 1). We chose two kinds of interpolations for rotation angles of the two intermediate segments, a quadratic one and a cubic one, and we instructed the code to randomly pick up one of them as it moved from one magnet to the other. This approach in some sense provided a higher degree of smoothness than those followed in the first two models.

Since it is the average effect that most heavily influences the orbit, we subtracted the average α in each magnet from individual segmental rotations. This kind of simulation corresponds to an installation procedure in which the twist for each magnet would be determined by measurements, the average direction of B found and the magnet attempted to be installed in such a manner that the average B lies along the vertical direction as accurately as possible. Consequently, the failure to align the average B exactly with the vertical direction was described by the overall rotation with rms value being 1 mrad, discussed in the past. Now it was the deviation from the average B in each dipole which introduced a new kind of perturbation to the closed orbit.

The more each magnet is split into individual randomly rotated segments, the closer is its average α to 0, the better is the actual cancellation of individual effects when the integrated effect is evaluated, and the smaller is the impact on the closed orbit. Therefore, we expected Model 1, with less magnet splitting, to produce bigger orbit distortions for the same α_{rms} than Model 2, and we expected Model 3 to fare roughly about the same as Model 2, since the whole interpolation used to rotate the seven segments was determined by only four random numbers and not seven. Our expectations were fully confirmed by computer simulations.

To conclude this section, we would mention that we performed our simulations by subjecting all dipoles in the lattice to the twist, in all of the three models discussed above.

Results

Our initial simulations revealed several characteristics of the problem. First, the effects of magnet twist are important only in the vertical plane. In the horizontal plane they were barely noticeable, being of the second order in the twist angle $\alpha(s)$. Secondly, the local three–bump correcting scheme coped effectively with orbit distortions as long as one of the correctors did not reach its maximum integrated field strength $(B\ell)_{max} = 0.3$ T·m. Thirdly, demands on kick strengths in the vertical plane rose rapidly with the increase of rms values of the twist angle. Fourthly, once the correctors cannot supply any more the

kick strengths demanded by the scheme's algorithm, the quality of the correction degrades rather rapidly with the increase in α_{rms}.

As a result of the foregoing, we decided to determine the α_{rms} at which the correction scheme breaks down, for each model and for each random error sequence. Based on the breakdown values for α_{rms} we would then recommend tolerances as far as the magnet twist is concerned. Of course, other lattice errors which give rise to a distorted closed orbit were to be kept fixed throughout the simulation procedure.

In addition to adopting the three models, we had also to select a certain number of random error sets both for the twist and for the other errors we considered. With the three adopted models and with the twist the number of computer runs grew rapidly and that imposed severe restrictions on the number of random error sequences that we could realistically simulate. Our choice was three random error sequences for the twist alone, and with the three models of twist this meant nine possibilities per each sequence of random errors other than twist. We then chose two random number sequences for the errors other than twist. Based on the past experience, we chose one good sequence, with IX=17 as the seed for the random number generator, and one bad sequence generated by IX=91, as its seed. In the absence of twist the terms "good" and "bad" meant the following.

A good or favorable distribution meant that the orbit could be initially corrected with the sextupoles at their full strength. A bad or unfavorable distribution meant that the orbit could not be initially corrected with the sextupoles at their full strength. The reason was the crossing of the sextupoles by the distorted closed orbit which entailed tune shifts that drove the lattice toward integer tune values, thereby making it unstable before any correction could be applied. The strategy to handle unfavorable distributions in the past was first to reduce the sextupole strengths to 50% of their full values, then to correct the orbit and increase the sextupole strengths to their full values, for the second iteration of the correcting scheme. After that, the third iteration always sufficed.

As we already mentioned, we chose one good distribution (the seed for the random number generator: IX=17) and one bad distribution (IX=91) for twist unrelated lattice errors, and for each of the two we chose three twist random error sequences ($IX_T = 88, 21,$ 15). We then used these six combinations in each of the three modelings of twist. Needless to say, the fact that different models involved different amounts of magnet splitting, and subsequently different amounts of usage of a random number sequence for the twist, meant that the fact that in different models we used the same IX_T really did not have any special significance.

One of the very first characteristics we observed, once we had introduced the twist, was the fact that any sizable twist ($\alpha_{rms} \geq 5$ mrad) upset the previously successful strategy for dealing with unfavorable distributions of random errors (without a twist). Even to be able to establish the orbit, we had to turn the sextupoles off (a 50% reduction of their nominal strengths did not suffice). Then we corrected the orbit, turned the sextupoles on and applied the second iteration of the three–bump correcting scheme. In all of the cases, this second iteration then more than sufficed, unless the algorithm demanded kick strengths in excess of the available maximum. Furthermore, we found out that it was completely irrelevant whether the errors other than twist entered the simulation through a good or a bad distribution. Therefore, the presence of a sizable twist erased any differences between favorable and unfavorable sequences for errors other than twist. Also, this property did not depend on the model, showing thereby that in the vertical plane the effects of a twist of about 5 mrad rms value completely dominate over the effects of other errors.

Once the real simulation was underway, we followed a strategy by which we tried to find α_{rms} as closely to the correcting scheme's breaking point as possible, for each pair IX, IX_T and in each model. The breaking point was determined up to 0.5 mrad. That means that we found two values of α_{rms}; one α_{rms} slightly above the breaking point, i.e. with at least one corrector trying to exceed the maximum hardware capacity $(B\ell)_{max} = 0.3$ T·m, and another α_{rms} slightly below the breaking point. These two values differed by 0.5 mrad. The results for all three models are summarized in Table 1 and Table 2, which represent the cases IX=17 and IX=91, respectively.

The very first row in each table represents the case with no twist. These results appeared to be the same for all of the three models and they all agreed to at least eight significant digits with the results obtained by running the code on the lattice input with no twist splitting of magnets at all. This proved that the three lattices for the three models were correctly assembled and that a special algorithm, that takes care of the necessary correlation of $\Delta(B\ell)/B\ell$ errors and of achieving an overall rotation of the dipole split into segments, indeed performed well. With no twist, it is also obvious why the case IX=17 was good and IX=91 was bad. Both maximum and rms orbit distortions are much bigger for the IX=91 case. With the twist being present, this is still true in the horizontal plane, where the twist effects are of the second order in α_{rms}, but in the vertical plane everything depends on IX_T and not much on IX. Precise meanings of rows and columns in these two tables are given in the section describing tables. Here we would like to call the reader's attention to the fact that in each model there are two rows for the same IX_T, one for the case below the breaking point and another for the case above it. The scheme's failure to

6

effectively correct the orbit in the vertical plane, above the breaking point, is evident from the last column.

The two major results from the tables, namely α_{rms} below and above the breaking point are represented in Figure 5. This figure directly represents the dependence of the three–bump correcting scheme's breaking point on the model and random error sequences in question. A block positioned between two α_{rms} values in the figure means that the breaking point was between these two values of α_{rms}. The numbers in the blocks are the IX_T seeds for the twist sequences of random errors. The numbers corresponding to the non–twist IX=91 are underlined, whereas those corresponding to the IX=17 case are not.

A look at Figure 5 reveals the following features. The qualitative predictions of Model 2 and Model 3 are very similar. The six breaking points, for the six different combinations of random error distributions, are fairly uniformly distributed between $\alpha_{rms} = 5.5$ and $\alpha_{rms} = 12.0$ mrad for Model 2 and between 6.0 and 11.5 mrad for Model 3. For Model 1, the crudest one in our simulation program, the picture is slightly different. The breaking points occupy the space between 4.5 and 7.0 mrad, with a somewhat denser gathering between 6.0 and 7.0 mrad. Apparently, the crudeness of the model, i.e. its magnet splitting into only two parts, does not make provision for appreciable cancellations of the twist effects within each magnet and consequently the overall effect tends to be more pronounced. Hence, the correcting scheme's breakdown tends to occur for smaller values of α_{rms}.

Based on these results, we recommend rejection of any magnet whose α_{rms}, the rms value of the twist angle, exceeds 3.0 mrad. With 3.0 mrad we are still relatively far from the worst case we found, i.e. the scheme's breakdown at 4.5 mrad. At the value of 3.0 mrad, the maximum kick angle is 0.2448 mrad, which corresponds to the maximum integrated kick strength $(B\ell)_{max} = 0.21$ T·m, or 2/3 of the hardware capacity, at the top magnetic rigidity $B\rho = 850$ T·m. As a matter of fact, this safety margin is even greater since $\alpha_{rms} = 3.0$ mrad is even further away from the lowest breaking points in Model 2 or Model 3, which are in our opinion more realistic.

Conclusion

Even though the realization that magnet twist is a factor that must be considered caused some initial anxiety about its possible impacts on the dipole performance, the results of our investigation, as well as those of our colleagues, have proved that twist will not present a major obstacle to a good magnet performance. The maximum value of α_{rms} that we recommend to tolerate provides a sufficient safety margin, yet the condition is not so stringent that it would impose extra problems during magnet manufacturing or involve

heavy additional expenses. The important point is that the measurements yield the value of the average direction of the $\vec{B}$ field and that the magnets are installed in such a manner that this average direction lies as accurately as possible in the vertical plane. By achieving an installation error $\Delta\theta \leq 1$ mrad and $\alpha_{rms} \leq 3$ mrad, we can be sure that the orbit correcting scheme will work well with the presently adopted hardware.

Table 1. Various characteristics of orbit distortions in the presence of magnet twist. The seed for the sequence of random errors other than twist: IX=17.

Seed IX_T	α_{rms} mrad	Kstr. (max)	AHL	$X_u{}^\circ$ (Extr./rms)	X_c (Extr./rms)	$Y_u{}^\circ$ (Extr./rms)	Y_c (Extr./rms)
	0.0	0.1522	N	91.059/21.449	-0.007/0.002	-47.807/16.255	0.000/0.000
88	6.0	-0.3368	N	91.037/21.381	-0.019/0.006	-134.429/40.727	0.000/0.000
M 88	6.5	-0.3618	Y	91.045/21.375	0.009/0.002	-141.648/42.895	1.437/0.479
O D 21	6.0	0.3271	N	90.949/21.417	-0.031/0.009	-134.533/38.490	0.000/0.000
E 21	6.5	0.3576	Y	90.922/21.409	-0.047/0.012	-142.223/40.881	-1.216/0.381
L 15	5.0	0.3208	N	91.775/21.662	-0.052/0.016	88.875/21.120	0.000/0.000
1 15	5.5	0.3509	Y	91.929/21.708	-0.063/0.019	99.770/25.126	-0.142/0.044
88	11.5	0.3418	N	92.521/21.769	0.073/0.021	-183.703/60.077	-0.002/0.000
M 88	12.0	0.3538	Y	92.642/21.796	0.070/0.021	-189.853/62.494	-0.575/0.197
O D 21	7.0	0.3335	N	90.942/21.409	0.020/0.006	118.310/32.478	0.000/0.000
E 21	7.5	0.3568	Y	90.918/21.401	0.022/0.007	127.308/35.432	-1.030/0.319
L 15	5.5	0.3453	N	91.054/21.446	-0.010/0.003	47.977/15.374	0.000/0.000
2 15	6.0	0.3629	N	91.062/21.448	0.012/0.004	53.036/15.984	2.037/0.639
88	8.0	0.3381	N	92.701/21.855	-0.041/0.013	-148.399/29.274	0.000/0.000
M 88	8.5	0.3608	Y	92.897/21.902	-0.059/0.018	-159.091/31.336	1.707/0.510
O D 21	7.5	0.3436	N	91.081/21.505	0.050/0.016	-194.315/61.003	-0.001/0.000
E 21	8.0	0.3586	Y	91.090/21.516	0.085/0.026	-205.930/64.988	-1.353/0.413
L 15	11.0	0.3485	N	91.655/21.512	0.068/0.018	-401.282/117.14	0.000/0.000
3 15	11.5	0.3656	Y	91.714/21.519	0.081/0.024	-417.599/121.95	2.339/0.744

The first row represents the case with no twist. The subsequent rows represent the cases with various twist related random seeds ($IX_T = 88, 21, 15$), in the three different models of the twist, below and above the breaking point of the correcting scheme, for each IX_T.

The meanings of the columns are as follows:
Col. 1 Seed for random numbers for the twist angle (IX_T).
Col. 2 rms value for the twist α_{rms}.
Col. 3 Maximum corrective kick strength (kick angle in milliradians).
Col. 4 Status of the kick angle (if Above Hardware Limits, AHL=Y).
Col. 5 Uncorrected horizontal displacement, Extreme/rms (in mm), with the sextupoles off.
Col. 6 Corrected horizontal displacement, Extreme/rms (in mm), with the sextupoles on (second iteration).
Col. 7 Uncorrected vertical displacement, Extreme/rms (in mm), with the sextupoles off.
Col. 8 Corrected vertical displacement, Extreme/rms (in mm), with the sextupoles on (second iteration).
Note: $(B\ell)_{max} = 0.3$ T·m corresponds to the kick angle of 0.35 mrad, at the top magnetic rigidity $B\rho = 850$ T·m.

9

Table 2. Various characteristics of orbit distortions in the presence of magnet twist. The seed for the sequence of random errors other than twist: IX=91.

Seed IX_T	α_{rms} mrad	Kstr. (max)	AHL	X_u° (Extr./rms)	X_c (Extr./rms)	Y_u° (Extr./rms)	Y_c (Extr./rms)
	0.0	0.0843	N	155.155/49.307	0.001/0.000	-132.318/34.645	0.000/0.000
88	6.0	0.3348	N	155.732/49.558	0.009/0.003	234.421/59.783	0.000/0.000
88	6.5	0.3588	Y	155.830/49.587	-0.011/0.004	242.945/61.942	-1.411/0.443
21	6.5	0.3387	N	154.578/49.202	-0.012/0.004	150.236/37.413	0.000/0.000
21	7.0	0.3692	Y	154.508/49.179	0.040/0.012	155.635/38.860	-3.138/0.982
15	4.5	0.3352	N	154.668/49.206	-0.050/0.016	48.262/15.208	0.000/0.000
15	5.0	0.3653	Y	154.547/49.160	-0.061/0.020	44.717/13.670	-2.381/0.738
88	11.5	-0.3391	N	157.337/49.642	-0.047/0.010	-116.548/40.760	0.000/0.000
88	12.0	-0.3512	Y	157.528/49.663	-0.048/0.010	-122.695/42.804	-0.187/0.060
21	8.5	0.3383	N	155.673/49.475	-0.022/0.006	-166.132/46.266	0.000/0.000
21	9.0	0.3615	Y	155.741/49.487	0.022/0.006	-175.511/48.674	-1.802/0.562
15	9.5	0.3493	N	154.312/49.354	-0.016/0.004	77.715/22.193	0.000/0.000
15	10.0	0.3669	Y	154.219/49.350	-0.024/0.008	77.445/22.170	2.718/0.852
88	6.0	0.3337	N	154.896/49.300	-0.013/0.004	-135.046/39.873	0.000/0.000
88	6.5	0.3563	Y	154.851/49.284	-0.017/0.006	-145.742/41.105	1.014/0.303
21	9.5	-0.3371	N	152.023/48.699	0.059/0.019	-352.922/100.13	-0.002/0.000
21	10.0	-0.3531	Y	151.672/48.619	0.061/0.019	-364.531/104.06	-0.489/0.156
15	9.5	0.3381	N	156.537/49.533	0.077/0.018	-307.227/98.43	0.000/0.000
15	10.0	0.3527	Y	156.697/49.552	0.088/0.020	-323.139/102.98	0.426/0.127

(Left margin labels: MODEL 1 for the first group, MODEL 2 for the second group, MODEL 3 for the third group.)

The first row represents the case with no twist. The subsequent rows represent the cases with various twist related random seeds (IX_T = 88, 21, 15), in the three different models of the twist, below and above the breaking point of the correcting scheme, for each IX_T.

The meanings of the columns are as follows:

Col. 1 Seed for random numbers for the twist angle (IX_T).
Col. 2 rms value for the twist α_{rms}.
Col. 3 Maximum corrective kick strength (kick angle in milliradians).
Col. 4 Status of the kick angle (if Above Hardware Limits, AHL=Y).
Col. 5 Uncorrected horizontal displacement, Extreme/rms (in mm), with the sextupoles off.
Col. 6 Corrected horizontal displacement, Extreme/rms (in mm), with the sextupoles on (second iteration).
Col. 7 Uncorrected vertical displacement, Extreme/rms (in mm), with the sextupoles off.
Col. 8 Corrected vertical displacement, Extreme/rms (in mm), with the sextupoles on (second iteration).

Note: $(B\ell)_{max} = 0.3$ T·m corresponds to the kick angle of 0.35 mrad, at the top magnetic rigidity $B\rho = 850$ T·m.
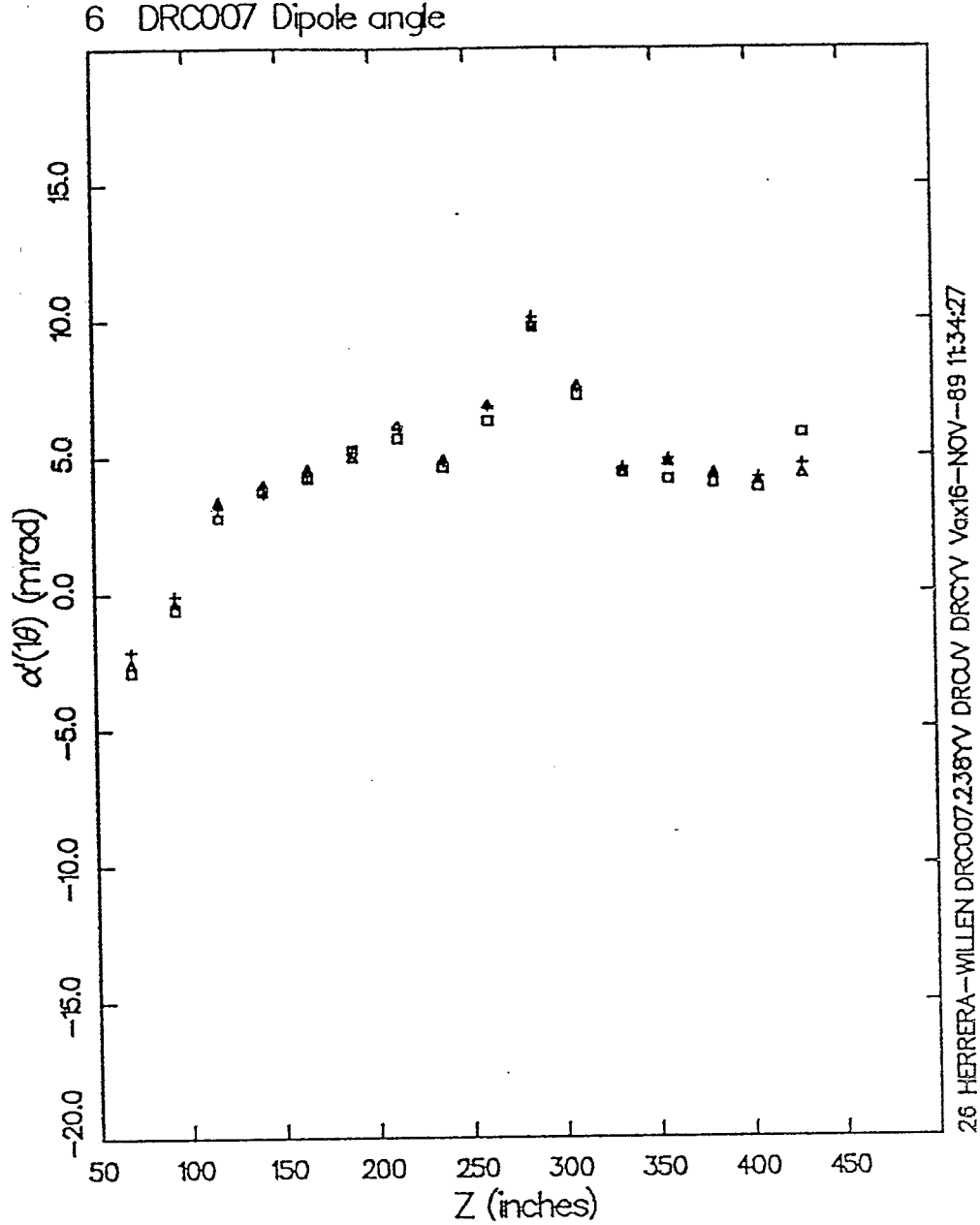
Fig. 1. This plot represents the directional deviation (Dipole angle) of the dipole field component for the RHIC dipole DRC007, as found by the BNL Magnet Testing Group and reported in their techical note MTG–439. The dipole field component is tilted from a conveniently fixed direction (0.0 on the diagram) by an angle α which varies over the range from about -3.0 to about 7.5 (10.0 if the middle cusp is counted) milliradians. The rms value of α, determined crudely by reading off the values from the 16 available points on the diagram, is approximately $\alpha_{rms} = 2.9$ mrad. This means that this magnet would still pass the acceptance test ($\alpha_{rms} \leq 3.0$ mrad) which we propose in this note, as a result of our simulations.
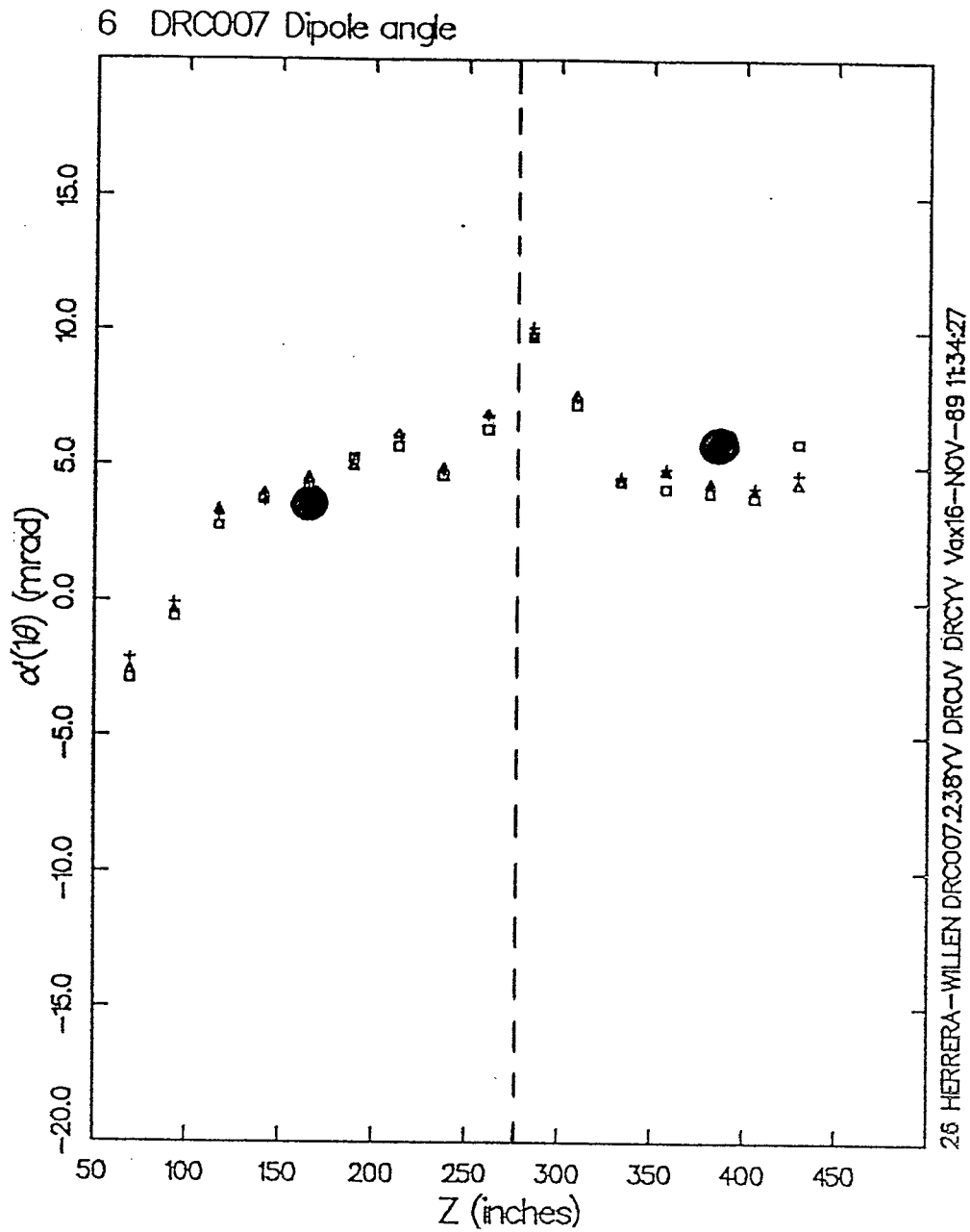
11

6 DRC007 Dipole angle

Fig. 2. This plot represents a sketch of the Model 1 magnet splitting, overlaying the background of the DRC007 magnet measurements, with the two rotations trying to match the effects felt by the 16 measurements. The two rotations are represented by heavy dots.
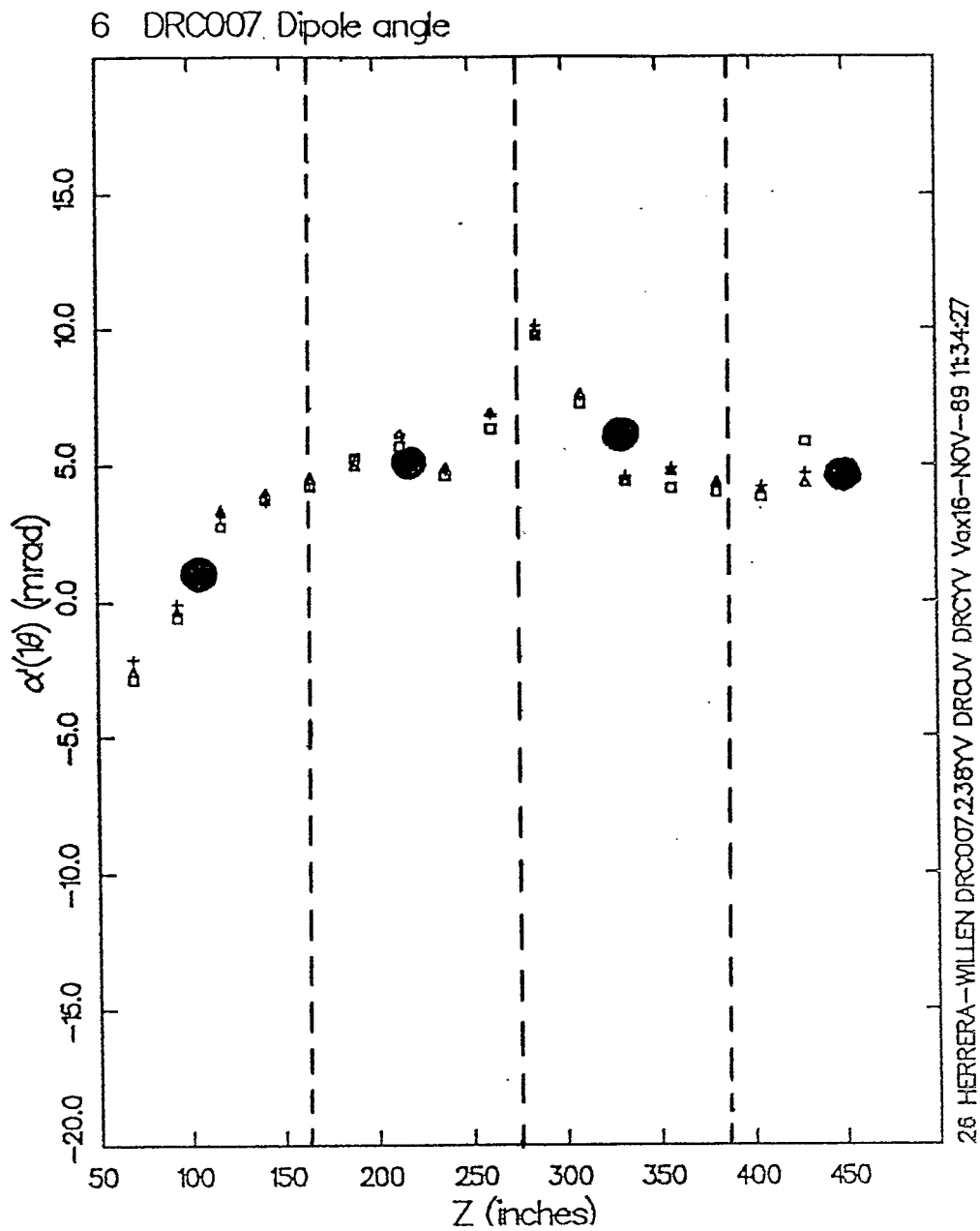
Fig. 3. This plot represents a sketch of the Model 2 magnet splitting, overlaying the background of the DRC007 magnet measurements, with the four rotations trying to match the effects felt by the 16 measurements. The four rotations are represented by heavy dots.
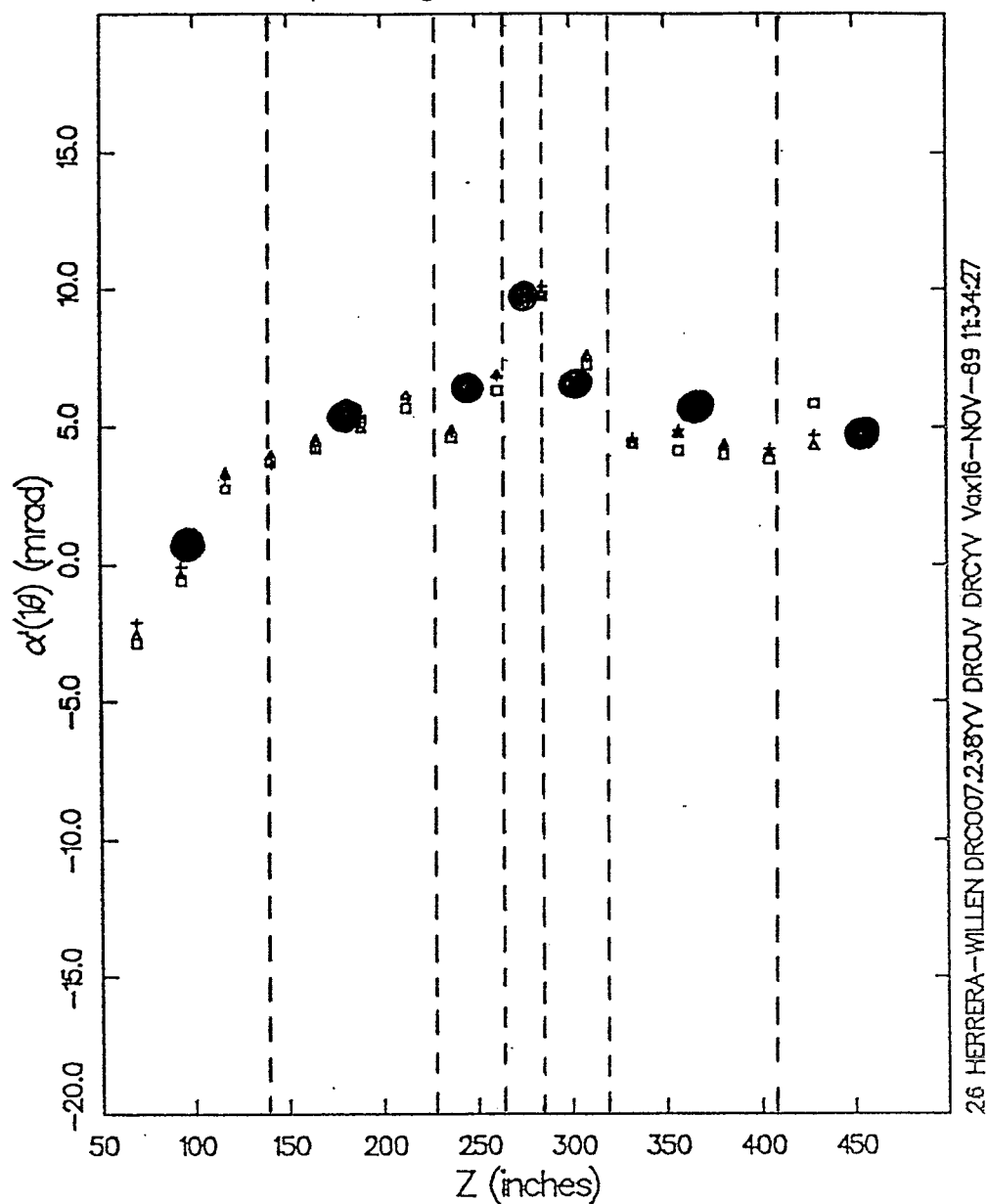
6 DRC007 Dipole angle

Fig. 4. This plot represents a sketch of the Model 3 magnet splitting, overlaying the background of the DRC007 magnet measurements, with the seven rotations trying to match the effects felt by the 16 measurements. The seven rotations are represented by heavy dots. This model apparently provides the highest degree of smoothness.
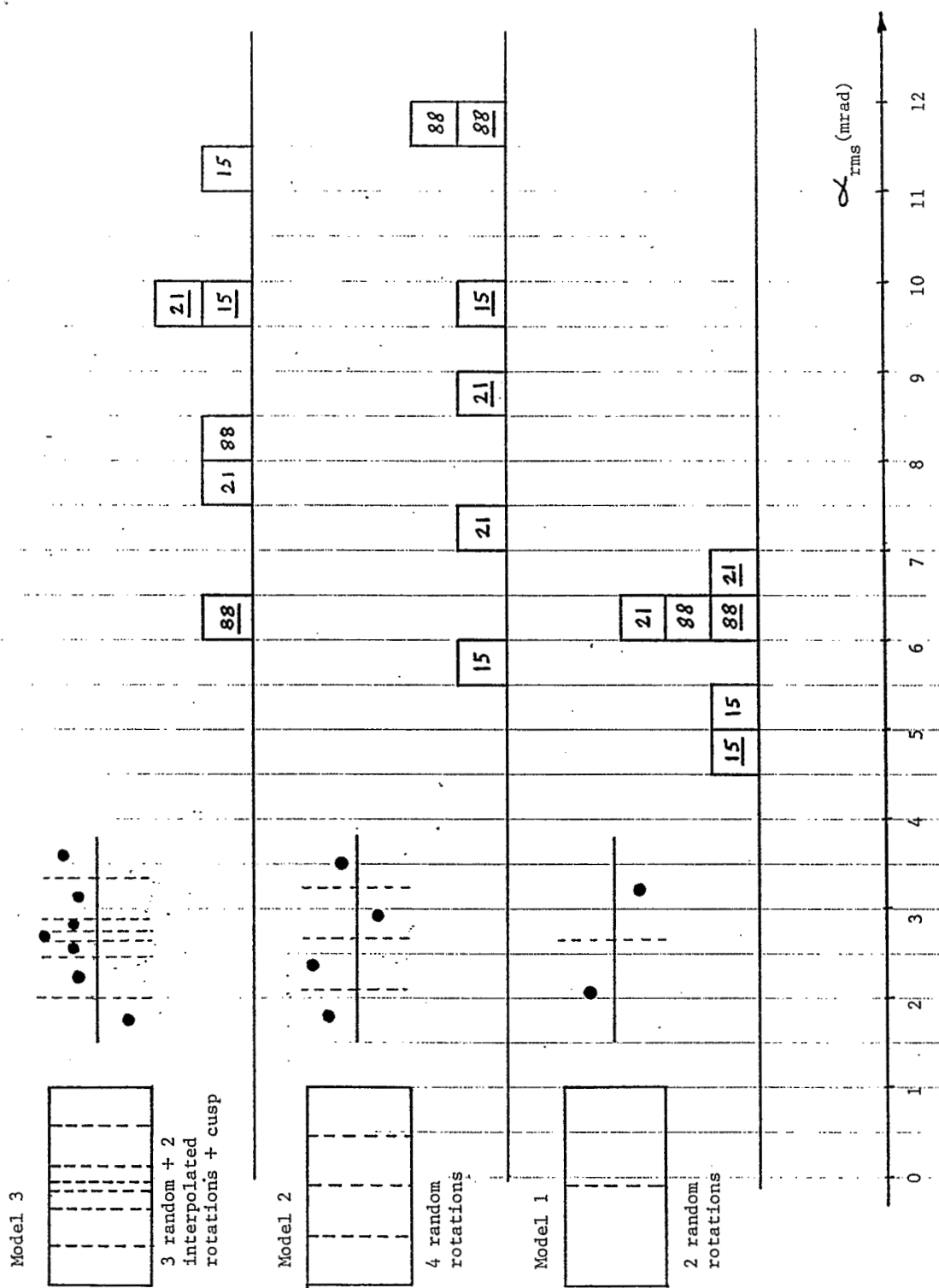
Fig. 5. Breaking points for the orbit correcting scheme for various random error distributions, as functions of α_{rms}, the twist angle rms value. All three twist models are shown. On the left, there is a sketch of the magnet splitting for each particular model. This sketch is then followed by a small diagram showing how the segmental rotations represent the twist in each model. On the main diagram, a block positioned between two values in the figure means that the breaking point was between these two values of α_{rms}. The numbers in the blocks are the IX_T seeds for the twist sequences of random errors, underlined if the non–twist IX=91.